

Size Dependence on Solubility for Controlled Continuous Crystallizations

Ingo H. Leubner

Crystallization Consulting, 35 Hillcrest Drive Penfield, NY 14526, USA

ileubner@crystallizationcon.com

Abstract

For crystallizations in continuous CSTR (MSMPR) crystallizers, a quantitative model correlating the average crystal size with reaction conditions is presented. This model is based on the balanced nucleation and growth (BNG) theory. In the present paper, the size dependence on crystal solubility is derived and experimentally supported. For silver chloride as a model system, the solubility was varied from 0.81 to 8.3E-06 mole/l (60C, 3.0 min residence time). The correlation coefficient between model and crystal sizes (0.34 - 0.52 μm) was 0.9996. The model calculated the average maximum crystal growth rate (8.5 A/s) and the ratio of critical to average crystal size (0.39). It further calculated the sizes of nascent, newly formed, crystals (0.13 – 0.30 μm), critical crystal sizes (0.13 – 0.20 μm), and supersaturation ratios (1.0049–1.0075) for the experimental conditions. The model showed a reactant split ratio R_n/R_i (0.06 - 0.26) of incoming reactant addition rate, R_0 , into growth (R_i) and nucleation streams (R_n). The average crystal size is predicted to be independent of reactant addition rate, suspension density, and reaction volume. This was experimentally confirmed for variation of suspension density from 0.05 to 0.4 mole/l (average crystal size 0.337 +/- 0.009 μm). The crystal number increased linearly with suspension density. The BNG based continuous crystallization model thus correctly predicted and quantitatively correlated the crystal size-dependence on solubility and suspension density in the CSTR crystallizer without the need for arbitrary adjustable parameters. It allowed determining important reaction parameters that were previously not accessible.

I. Introduction

In crystallization processes and for the control of crystal size, growth, and design, the control of crystal nucleation is a crucial first step in research, product development, and manufacturing. For this purpose, a balanced nucleation and growth model (BNG) was developed.¹ The BNG model is the basis, which provides a fundamental model to control crystal nucleation and growth in continuous crystallizations. Experimental results are presented which support the model.

Continuous production of materials is an important industrial process. For continuous chemical processes and crystallizations, the controlled continuous stirred tank reactor (CSTR), or mixed-suspension, mixed-product-removal (MSMPR) system and the stop-flow system are preferred for controlled crystallizations. The present work concentrated on the CSTR (MSMPR) crystallizer and on the effect of varying crystal solubility on the crystal size.

To obtain consistent crystalline products, it is important to understand the relationship between the engineering variables and the properties of the precipitate. Important crystallization engineering variables are reaction volume, temperature, crystal solubility, material flow and reactant addition rates, residence time, and the presence of ripeners² and restrainers³, suspension density, stirring/mixing, and the balanced withdrawal of reacted and unreacted material. The precipitate properties are related to the composition of the precipitate, average crystal size, and crystal size distribution (CSD).

Related to the product properties are reactions taking place in the reactor, the formation of crystals (nucleation rate), their growth (growth rate), and the mechanisms of crystal formation, homogeneous, heterogeneous, or secondary nucleation.

Different but complementary steady - state theories of crystallization in the continuous stirred tank reactor (CSTR, or mixed-suspension, mixed-product-removal, MSMPR) crystallizer have been proposed.^{4, 5, 6, 7}

The Randolph-Larson Model

Bransom et al., and Randolph and Larson (R-L) modeled the correlation between crystal size distribution, crystal growth rate, and residence time (equation (1)) at steady state, by using a mass-balance model.

	$n_x = n_0 \exp(-L_x/\tau G)$	(1)
--	-------------------------------	-----

Here, $n_x = Z_x / \text{cm}^3$, where, n_x is number population density of crystals of size L_x per reaction volume; Z_x is the number of crystals of size L_x ; $n_0 = Z_0 / \text{cm}^3$ ('cm' represents the crystal size, 'cm³' the normalization of reaction volume), number of crystals, Z_0 , of size L_0 nucleated per time and volume; L_x = crystal size of defined crystal size populations; $G = dL/dt$

= growth rate; and τ = residence time, determined by the reaction volume divided by material flow rate (input or output).

Randolph and Larson gave an extensive review of this model.⁶ The underlying model (equation (1)) is based on continuous nucleation of infinitely small crystals followed by growth. The model parameters are the residence time, τ , and crystal growth rate, G . The model (equation (1)) does not relate crystal size and distribution to reaction variables like temperature, crystal solubility, and suspension density. To overcome this restriction, additional concepts and equations were introduced.⁶ These include birth and death rates, which represent the formation and destruction of particles in the reaction mixture. The growth rate, G , is a function of addition rate and can be expressed by the mass balance equation (2).

	$G = \frac{dL}{dt} = \frac{RV_m}{3.0k_v ZL^2}$	(2)
--	--	-----

Here, L is the crystal size, R is the addition rate (mole/s), V_m is the molar volume (cm^3/mole), k_v is the volume conversion factor which converts L to the crystal volume, and Z is the number of crystals in the reaction mixture. For polydisperse reaction mixtures, Z is replaced by Z_x , L by L_x , and it is necessary to integrate over x . G is also a function of supersaturation, which frequently cannot be experimentally determined or used as control variable. For further details of the Randolph-Larson model, it is necessary to refer to the literature.⁶

Generally, n_x , n_0 , L_x , and G (equation (1), birth and death rates, supersaturation, and other R-L variables are not known a priori for continuous crystallization systems that are based on continuous nucleation and growth. Equation (1) is, however, well suited for the control of crystal growth and crystal size distribution of continuously seeded CSTR systems, where, the input of number and size of seeds (n_0 , birth rate) and the reactant addition rate for growth are quantitatively controlled.⁸

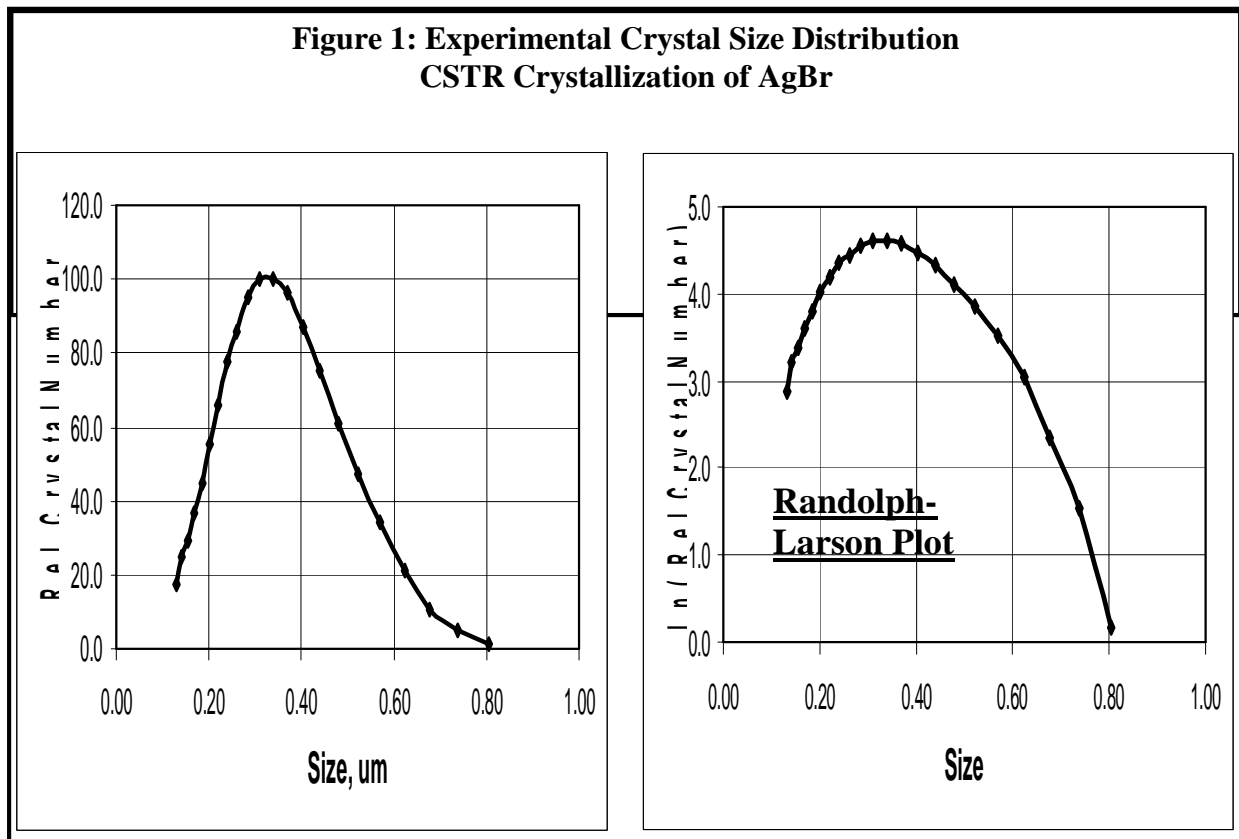
The present BNG model arrived from the necessity to predict the maximum size of crystals obtained in controlled continuous crystallizations in continuous stirred tank (CSTR, MSMR) reactors. The maximum crystal size is defined in this context as the size of the crystal population that has the highest number of crystals in the reaction mixture. For systems that do not deviate too much from monodispersity, this crystal size generally represents the general properties of the crystal size population.

II. The BNG Model for the CSTR System

The present alternate model for size control in continuous crystallizations is based on the balanced nucleation and growth (BNG) model. This model quantitatively correlates the maximum crystal size at steady state with the precipitation temperature, product solubility, and reactant addition rate (equation (14)). This model was supported by experiments where the residence time, τ , was varied.⁷

For controlled continuous crystallizations of silver halide in the CSTR system, a well-defined crystal size distribution is obtained at steady-state (Figure 1a). Re-plotting the size distribution using the guidance of equation (1) does not give the predicted linear plot. The cut-off for crystal size distribution is about 0.08 μm , and thus the increase in crystal number with crystal size is within the experimental sizing range. The lower crystal number at small sizes is difficult to bring in alignment with the prediction of equation (1), which predicts a steady decrease of crystal number with increasing crystal size.

For many product applications, e.g. photographic systems, the largest crystal size, L , dominates the critical product properties, e.g., photographic sensitivity. Thus, it became necessary to develop a model that correlates L with experimental control variables, like reaction addition rate, crystal solubility, and temperature. To relate the crystal size, L , to these experimental control parameters, a mass-balance model was designed that includes both nucleation and crystal growth (Figure 2).⁷



The BNG Model

In the BNG model (Figure 2:), the input addition stream, R_0 (e.g. mole/min), is split into a growth stream, R_i (size increase, to avoid confusion with R_g , the gas constant), and into a stream that is consumed for nucleation, R_n . The sum of R_i and R_n is, of course, equal to R_0 (equation (3)). To simplify modeling, full conversion of incoming material into crystals is assumed.

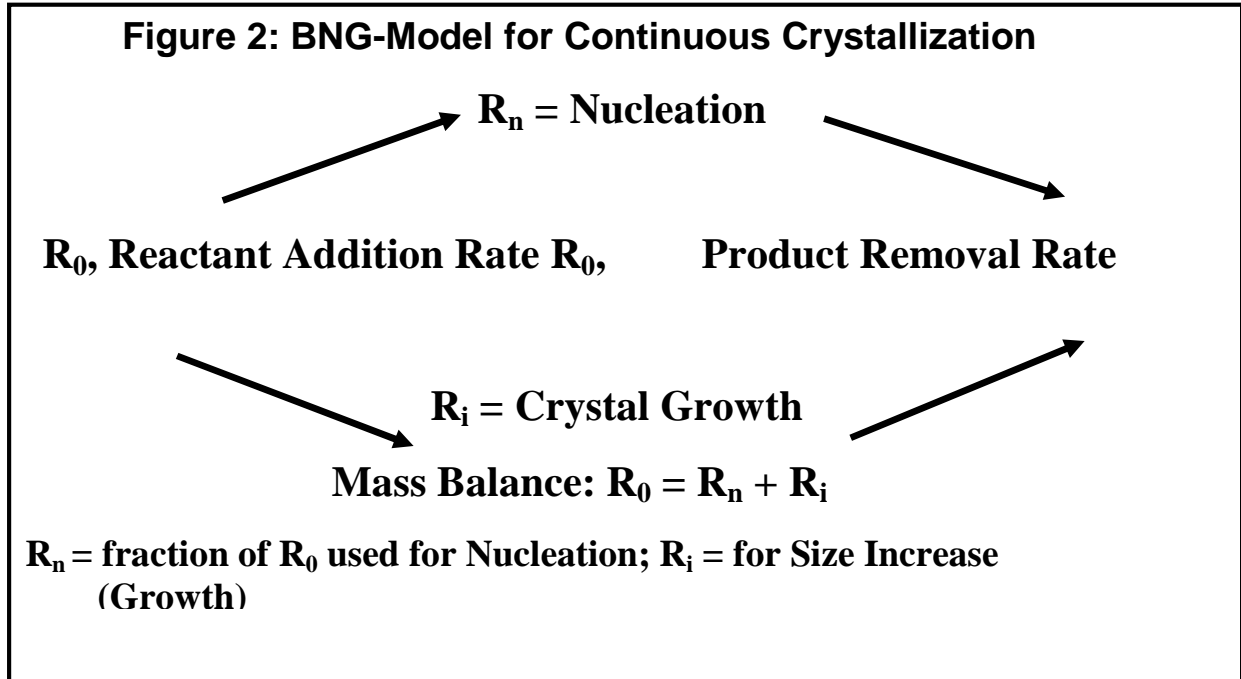


Figure 2:	BNG-Model for Continuous Crystallization
-----------	--

	$R_0 = R_n + R_i$	(3)
--	-------------------	-----

In the following, analytical equations to express R_n and R_i are introduced.

Figure 1	Experimental Crystal Size Distribution and R-L plot: CSTR Crystallization of AgBr
----------	---

Crystal Growth

The reactant stream for crystal growth, R_i , was derived from equation (2) since at steady-state the number and size distribution of the crystals is known and constant. In continuous crystallizations with continuous nucleation, G is equal to G_m , the maximum growth rate of the crystal population. The maximum growth rate of a crystal system is defined by the growth rate

where new crystals begin to form in the reaction mixture by homogeneous nucleation ('renucleation'). Crystal renucleation is inherent in continuous crystallization, since continuous formation of new crystals (renucleation) is necessary to replace the crystals that are leaving the reaction mixture. Renucleation was quantitatively modeled for batch crystallization where the reactant addition rate exceeded the maximum growth rate of the crystal population.⁹

The crystal population in the CSTR crystallizer is represented by Z the number of crystals of size L in the reaction mixture. For convenience and clarity of derivation, representative Z and L values are taken to represent the crystal population. In the present work, the crystal size with highest crystal number was chosen, and Z calculated from the mass balance in the reactor.

For highly soluble materials, the product stream leaving the reaction mixture may contain non-crystallized and unreacted material ($R_0 = R_n + R_i + R_u$). The fraction, R_u , must be subtracted from the input/output stream to obtain an effective R_0' stream that only contains R_i and R_n . For the present derivation, products with low solubility are considered, and R_u was considered negligible.

The number of crystals formed during one residence time, Z_t , is given by the mass balance equation (4)

	$Z_t = \frac{R_0 V_m \tau}{k_v L^3}$	(4)
--	--------------------------------------	-----

For crystal growth, equation (2) is applied to R_i and Z_t and solved for R_i (equation (5))

	$R_i = \frac{3.0k_v G_m Z_t L^2}{V_m}$	(5)
--	--	-----

Inserting Z_t from equation (4) into equation (5) leads to an analytical equation for R_i (equation (6))

	$R_i = \frac{3.0G_m R_0 \tau}{L}$	(6)
--	-----------------------------------	-----

Strong and Wey derived an analytical expression for the maximum growth rate and its dependence on material and reaction properties (equations (7) and (8)).¹⁹ This equation is part of the derivation of the BNG nucleation model.¹

	$G_m = \left[\frac{dr}{dt} \right]_{\max} = \frac{2\gamma V_m C_s K_i (1.0 - L^*/L)}{R_g T L^* (1.0 - \varepsilon/L)}$	(7)
Where	$\varepsilon = K_i / DV_m$	(8)

New variables are: γ , the crystal surface energy (erg/cm²), C_s , the crystal solubility, K_i , the surface integration constant, L^* , the critical crystal size (which has equal probability to grow or dissolve under the reaction conditions), R_g , the gas constant, T the temperature (K), and D the diffusion constant for the reactant under the reaction conditions (cm²/s).

Crystal Nucleation

The number of crystals that are nucleated, Z_n , is equal to the number of crystals leaving the system (k_v is the volume conversion constant for L).

	$Z_n = \frac{R_0 V_m}{k_v L^3}$	(9)
--	---------------------------------	-----

According to the balance nucleation and growth model, the number of crystals nucleated also is a function of R_n (equation (10)).¹²

	$Z_n = \frac{R_n T}{C_s} \left[\frac{R_g}{2k_s \gamma DV_m \Psi} \right]$	(10)
Where	$\Psi = L/L^* - 1.0$	(11)
And	$L^* = \frac{L}{\Psi + 1.0}$	(12)

Equation (9) is inserted into equation (10) and is solved for R_n (equation (13)).

	$R_n = \frac{R_0 C_s}{TL^3} \left[\frac{2k_s \gamma DV_m^2 \Psi}{k_v R_g} \right]$	(13)
--	---	------

The Model

The results for R_i and R_n (equations (5) and (13)) are inserted into equation (3) ($R_0 = R_n + R_i$), which leads to equation (14).

	$k_v R_g L^3 T - 2k_s \gamma DV_m^2 \Psi C_s - 3k_v R_g G_m L^2 T \tau = 0$	(14)
--	---	------

G_m and Ψ may be functions of T , C_s , and τ . The complexity of equation (14) does not allow to determine both G_m and Ψ for a single reaction condition. The determination of G_m and Ψ for a given variable/size combination may be achieved if the aim condition is bracketed by symmetrical condition. Average values of G_m and Ψ can be calculated for a set of adjacent determinations, and trends of these parameters may be obtained. Because of the limited number of experiments available in the present and previous work, average values of G_m and Ψ were obtained.

A main feature of equation (14) is the absence of the reaction volume, reactant addition rate, and suspension density. This suggests that these factors do not affect the crystal size. This is in contrast to equation (1), where the reaction volume is included. The results of the experiments will show agreement with the predictions of equation (14) of the BNG model.

Supersaturation Ratio

Knowledge of Ψ allows calculating the critical crystal size, L^* (equation (12)), and from this the supersaturation ratio in the system (equation (15)).

	$S^* = \frac{C - C_s}{C_s} = 1.0 + \frac{2.0 \gamma V_m}{R_g TL^*}$	(15)
--	---	------

Here, S^* is the supersaturation ratio at steady-state; $(C - C_s)$ is the supersaturation; C is the reactant concentration (including supersaturation); and C_s is the crystal equilibrium solubility. Thus, the supersaturation ratio, S^* , the solubility C , and the supersaturation, $(C - C_s)$ can be calculated from Ψ , the average crystal size, L , and critical crystal size, L^* , and the equilibrium solubility, C_s . (A glossary of terms is given in Table 11).

Reactant Split, R_n and R_i

The BNG CSTR model is based on a split of the reactant input stream, R_0 , into a nucleation stream, R_n , and a growth stream, R_i (Figure 2:). The ratio $R_{n,i}$ ($=R_n/R_i$) is obtained by dividing equation (13) by equation (5), which gives equation (16).

	$R_{n,i} = \frac{R_n}{R_i} = \frac{2k_s \gamma D V_m^2}{3k_v R_g} * \frac{\Psi}{G_m} * \frac{C_s}{T\tau} * \frac{1.0}{L^2}$	(16)
--	---	------

In equation (16), all data are available, and thus R_n/R_i was calculated. By combining equations (3) and (16), R_n and R_i were calculated as a function of R_0 (equations (17) and (18)).⁷

	$R_n = R_0 / (1.0 + 1.0 / R_{n,i})$	(17)
	$R_i = R_0 / (1.0 + R_{n,i})$	(18)

Nascent Nucleus Size

‘Nascent nuclei’ are defined as the stable crystals of size L_n that are formed (nucleated) during steady state to replace the crystals leaving the reaction mixture.

The model and the experimental results allow calculating the size L_n of the nascent nuclei for the different reaction conditions. For this purpose, L_n is given by equation (19).

	$L_n^3 = \frac{R_n V_m}{k_v Z_n}$	(19)
--	-----------------------------------	------

Back-substitution of R_n (equation (17)) and Z_n (equation (9)) into (19) leads to equation (20).

	$L_n^3 = \frac{R_n}{R_0} L^3$	(20)
--	-------------------------------	------

The full analytical equation for L_n is obtained by stepwise back substitution of R_n/R_i (equation (21)).

	$L_n^3 = \frac{2k_s \gamma D V_m^2 C_s \Psi}{3k_v G_m R_g T \tau L^2 + 2k_s \gamma D V_m^2 C_s \Psi} L^3$	(21)
--	---	------

Because of its simplicity, equation (20) was used for the calculations.

Summary of Model

Equation (14) models systems with homogeneous nucleation and diffusion controlled growth, which was established for the present AgCl model system.¹² Derivation of an equation based on kinetically controlled growth is possible, but is not required for the present model system. Equation (14) is based on the BNG nucleation model, which has been confirmed for controlled double-jet batch precipitations.^{10,11,12} No assumptions of size-dependent growth are needed, since the underlying growth model includes this effect.^{12,19}

The model predicts the correlation of the maximum crystal size with residence time, solubility, and temperature of the system. It allows determining the maximum growth rate, G_m ; the ratio of average to critical crystal size, L/L^* , the critical crystal size, L^* , the supersaturation ratio, S^* , the reactant split ratio of the fractions of the input stream used for nucleation and crystal growth, R_n/R_i ; and the size of the nascent nuclei, L_n .

The model predicts that the average crystal size is independent of reactant addition rate and suspension density, which was experimentally confirmed for the case of varying residence time, τ . The maximum crystal size is a non-linear function of the residence time where the crystal size has a positive value at zero residence time (plug-flow condition). The model may be extended to systems containing ripening agents or growth restrainers, and systems where growth and nucleation are kinetically, heterogeneously, or otherwise controlled.⁷

III. Size Control by Crystal Solubility

The Solubility Model

Solving Equation (14) for the crystal size, L , results in a highly complicated solution as a function of the reaction variables, which is of little practical use. Thus, equation (14) was solved to equation (22) to correlate solubility, C_s with crystal size, L . The same method was previously applied to model the correlation between residence time and crystal size.⁷

	$C_s = \left(\frac{k_v R_g T}{2k_s \gamma D V_m^2 \Psi} \right) (L^3 - 3G_m \tau L^2)$	(22)
Limits	$L \geq L_m, C_s \geq C_m$	

Equation (22) implies that the solubility can achieve a value of zero. However, Figure 4 shows that for AgCl the solubility goes through a minimum, C_m , and does not equal zero at any condition. In addition, the minimum size, L_m , is limited by the minimum solubility and only the minimum and larger sizes will be correctly modeled. Nevertheless, equation (22), allows to calculate a finite solubility for the condition $L=zero$.

To give a meaningful correlation for the case presented for AgCl, equation (22), the solubility for the condition $L=zero$, C_0 , must be added (equation (23)). This addition is forced by the correlation of solubility on the second and third orders of size and the solubility property of AgCl which does not include $C_s = zero$.

	$C_s = C_0 + \left(\frac{k_v R_g T}{2k_s \gamma D V_m^2 \Psi} \right) (L^3 - 3G_m \tau L^2)$	(23)
--	---	------

Equation (23) can be simplified by introducing an intermediate constant K (equations (24) and (25)). K is related to Ψ , which may be dependent on solubility. Thus, K may vary with solubility in relationship to Ψ . As discussed above, in the present experimental case, maximum growth rate, G_m and Ψ values are average values over the solubility range, and thus K is a constant for these considerations.

	$C_s = C_0 + KL^3 - 3G_m \tau KL^2$	(24)
Where:	$K = \frac{k_v R_g T}{2k_s \gamma D V_m^2 \Psi}$	(25)

To solve equation (24), a multivariate model was used to correlate crystal size to solubility

	$C_s = a_0 + a_1 L^3 + a_2 L^2$	(26)
--	---------------------------------	------

Here, a_0 represents the extrapolated solubility for $L=0$, C_0 , and a_1 is equal to K .

The fit of data to equation (24) provides K , from which Ψ is obtained by solving equation (25) for Ψ (equation (27)).

	$\Psi = \frac{k_v R_g T}{2k_s \gamma D V_m^2 K}$	(27)
--	--	------

The factors a_1 and a_2 were used to determine the average maximum growth rate, G_m (equation (28)).

	$G_m = \frac{a_2}{3\tau a_1}$	(28)
--	-------------------------------	------

Two limiting conditions can be derived from equation (22). The first is extrapolation to zero solubility (equation (29)). This approximation is only allowed if C_s experimentally approaches zero. Under these conditions (which are not met by the solubility properties of AgCl), this extrapolation indicates that the size would have a limiting value for zero solubility.

For the AgCl system, the lowest solubility is greater than zero and thus for the minimum solubility condition a size larger than L_0 is predicted.

	$L \rightarrow L_0 = 3G_m\tau$	(29)
--	--------------------------------	------

Another extrapolation is obtained for the condition given in equation (30).

	For $L \gg 3G_m\tau$	(30)
	$L^3 = \frac{2k_s\gamma DV_m^2\Psi}{k_v R_g T} * C_s = C_s / K$	(31)

This extrapolation (equation (31)) predicts that at large crystal sizes (as defined), L increases linearly with solubility.

Solubility

The solubility of crystals is given by the sum of the concentrations of all soluble species in solution that contain the reaction-determining ion, and which participate in the growth of the crystals. In the case of silver chloride, the precipitation is generally performed with chloride excess, so that the silver ion is the reaction-determining ion. Under these reaction conditions, the concentration of growth determining silver ion, the solubility of the AgCl crystals, C_s , is given by the concentrations of free silver ion, of silver chloride molecules in solution, and of silver-chloride, $AgCl_m^{1-m}$ complexes in solution as shown in equation (32).

	$C_s = [Ag^+] + [AgCl] + [AgCl_2^-] + [AgCl_3^{2-}] + [Ag_4^{3-}]$	(32)
--	--	------

The necessary constants to calculate the concentrations of these species are available from the literature and are compiled in Table 1.^{13, 14}

Table 1		
Constants for AgCl Solubility Calculation		
Component	K_{m,n}	ΔH
	(25C)	(kcal/mole)
[Ag ⁺]	10 ^{-pAg}	
[AgCl]	10 ^{-3.3}	-2.7
[AgCl ₂ ⁻]	10 ^{-5.25}	-3.9
[AgCl ₃ ²⁻]	10 ^{-5.7}	-5.8
[AgCl ₄ ³⁻]	10 ^{-5.4}	-13.9
$K_{sp} = [Ag^+][Cl^-]$	$K_{m,n} = \frac{[Ag^+]^m [Cl^-]^n}{[Ag_m Cl_n]^{m-n}} ; n=1$	
$\log K_{sp} = -(3206 \pm 42) / T + (1.17 \pm 0.14)$		
$T(K) = 273.15 + \text{degC}$		

Table 1	Constants for Solubility Calculations of AgCl
----------------	---

(Note: because of their size, all Tables are compiled at the end of the paper)

IV. Experimental

The experimental design for a standard precipitation is shown in Table 2. Variations from these conditions are apparent from Table 3. The steady state for crystals size and size distribution is only established after eight to twelve residence times, and the samples for size determination were pulled after twelve residence times.¹⁵ Longer reaction times, up to fifty residence times, did not show significant changes from these results. The experimental results are listed Table 3.

Table 2	Experiments: CSTR Precipitation of AgCl
Table 3	Summary of Experimental Results: Crystal Size and Number

Table 2	
Reference CSTR Precipitation Procedure for AgCl	
300 ml Reaction Volume (CSTR Crystallizer)	
2.4% Gelatin in distilled Water	
60 degree C	
EMF = 170mV, silver vs. silver/silver chloride (4.0N KCl) reference electrode*	
3.0 min Residence time	
10 ml/min Reactant Flow Rate (AgNO₃, NaCl)	
1.0 Mole/L Reactant Concentration	
80 ml/min Gelatin Flow Rate	
0.10 Mole/L AgCl Suspension Density	
Samples were collected after 12 residence times	
Crystal Size Analysis by Joyce-Loebl Disc Centrifuge	
The solubility was adjusted with sodium chloride to aim pAg	
*pAg = $\frac{(599 - mV) - (T - 25) * 0.129}{(273 + T) * 0.198}$	T= degC, mV= EMF

Table 3						
Experimental Results: Crystal Size and Number						
pAg	Reaction Volume mL	Reactant Concentr. Mol/L	Reactant Flow Rate mL/min	Suspension Density M/L	Size cel μm	Crystal Number $Z \cdot E+14$
7.8	300	1.0	10	0.100	0.516	0.19
7.1	300	1.0	10	0.100	0.399	0.41
6.4	300	0.5	10	0.050	0.327	0.37
6.4	600	1.0	20	0.100	0.337	0.68
6.4	300	1.0	10	0.100	0.350	0.60
6.4	300	2.0	10	0.200	0.331	1.42
6.4	300	3.0	10	0.300	0.333	2.10
6.4	300	4.0	10	0.400	0.344	2.55
5.9	300	1.0	10	0.100	0.353	0.59
5.4	300	1.0	10	0.100	0.369	0.52

The solubility was varied by adjusting the pAg ($-\log [\text{Ag}^+]$) in the reactor with sodium chloride. The pAg, which represents the activity of free silver ions in solution, was measured via the electromotive force (EMF) vs. a reference electrode as indicated in Table 2. The size and size distribution was determined using a Joyce-Loebl disk-centrifuge system.¹⁶ The reported sizes, which are given in equivalent circular diameter, were converted to cubic edge length by multiplying with the geometric factor 0.86.

V. Results

Suspension Density

Equations (22) and (23) imply that the crystal size is independent of reaction addition rate suspension density, and reaction volume. To check this prediction, the addition rate was varied from 0.005 to 0.04 mole/min for fixed conditions at a pAg 6.4 and solubility of $8.1 \cdot 10^{-5}$ mole/l.

The suspension density varied between 0.05 and 0.4 mole/l. The results are compiled in Table 4 and plotted in Figure 3.

The average crystal size is 0.337 ± 0.0085 μm cubic edge length (cel). The standard deviation of 0.0085 μm is within the expected experimental error of the variability of experiment and size determination. This confirms the model prediction that the variation of addition rate and suspension density under otherwise constant reaction conditions does not significantly change the average crystal size.

A possible reactor volume effect was tested for the 0.1 mole/l suspension density condition. Crystal sizes of 0.350 and 0.337 μm and crystal number (0.60 and 0.68 E+14 crystals) for the experiments with 300 ml and 600ml reaction volume are the same within the experimental error. If the reaction volume would control the crystal number, 1.2 E14 (instead of 0.68E+14) crystals would be predicted for the 600ml reaction volume. This supports the model prediction that the reaction volume does not significantly affect crystal size and crystal number.

Table 4	Suspension Density Variations (at pAg6.4): Crystal Size and Number
----------------	--

Table 4				
Suspension Density Variations at pAg6.4 : Crystal Size and Number				
Reactant Concentr.	Reaction Volume	Suspension Density	Crystal Size cel	Crystal Number
Mole/l	ml	Mole/l	μm	Z*E14
0.05	300	0.05	0.327	0.37
0.10	600	0.10	0.337	0.68
0.10	300	0.10	0.350	0.60
0.20	300	0.20	0.331	1.42
0.30	300	0.30	0.333	2.10
0.40	300	0.40	0.344	2.55

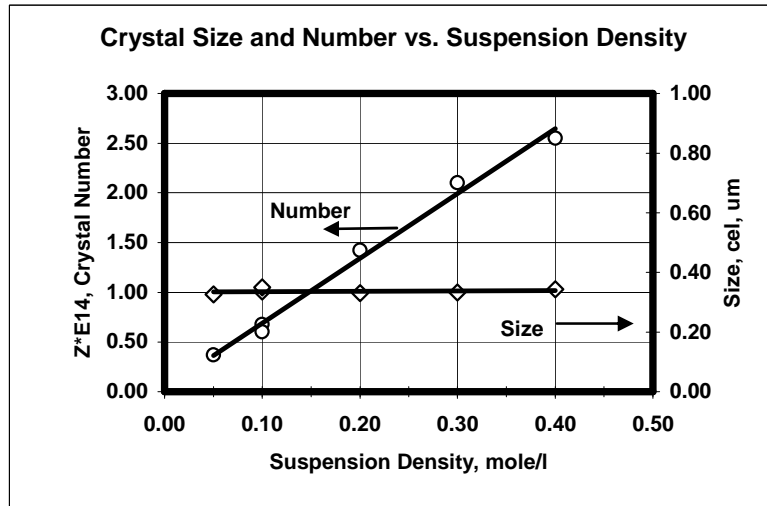


Figure 3

Crystal Size and Number vs. Suspension Density

Figure 3 shows that while the crystal size is independent of suspension density, the crystal number increases linearly with suspension density (equation (33)).

	$Z = (6.66 \pm 0.087)10^{14} * \text{SuspensionDensity(mole /l)}$	(33)
	All error limits equal one standard deviation; $R^2 = 0.9956$	

Size-Solubility Correlation

Equation (22) predicts that in the CSTR crystallizer the crystal size depends on the solubility and the crystal number is varied by varying the suspension density. In contrast, for batch precipitations, the crystal number depends on the solubility, and the crystal size is a function of the amount of precipitated mass.¹⁷

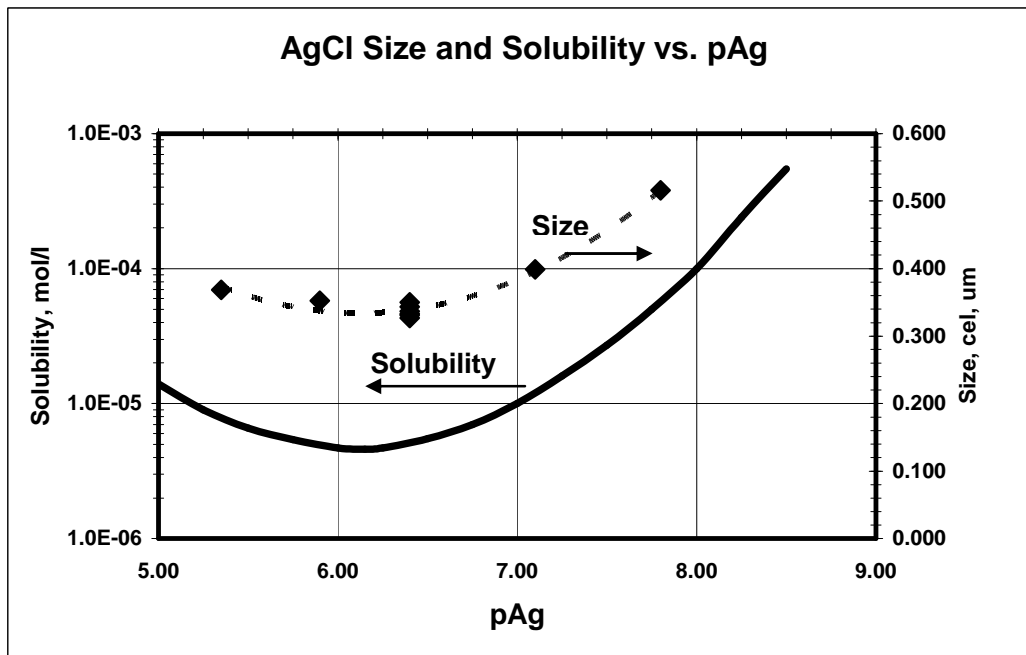


Figure 4	AgCl Solubility and Crystal Size vs. pAg (-log[Ag ⁺])
----------	---

In Figure 4, crystal size and solubility are plotted vs. pAg. This plot shows that crystal size and solubility are correlated. For instance, both solubility and crystal size go through a minimum at about pAg6.4, and are higher at lower and higher pAg.

To derive the correlation between size and solubility from the BNG model, the experimental data in Table 3 were analyzed using multivariate analysis according to equation (26). According to equation (24), a₀, is equal to the condition where L=zero. The results of the modeling are shown in equation (34). The standard deviations and the correlation coefficient, R² = 0.9996, indicate excellent correlation of the data with the model.

$C_s = (44.4 \pm 5.53) * 10^{-6} + (2.607 \pm 0.155) * 10^9 L^3 - (1.199 \pm 0.0996) * 10^5 L^2$	(34)
L (cm) cubic edge length (cel), C _s (mole/l)	

The plot of the experimental data and the modeling fit, size vs. solubility, is shown in Figure 5. The plot is in agreement with the model, which predicts that at low concentrations the size does not approach zero (equation (29)). Further, as predicted by the model, the correlation approaches linearity with solubility at larger sizes (equation (30)).

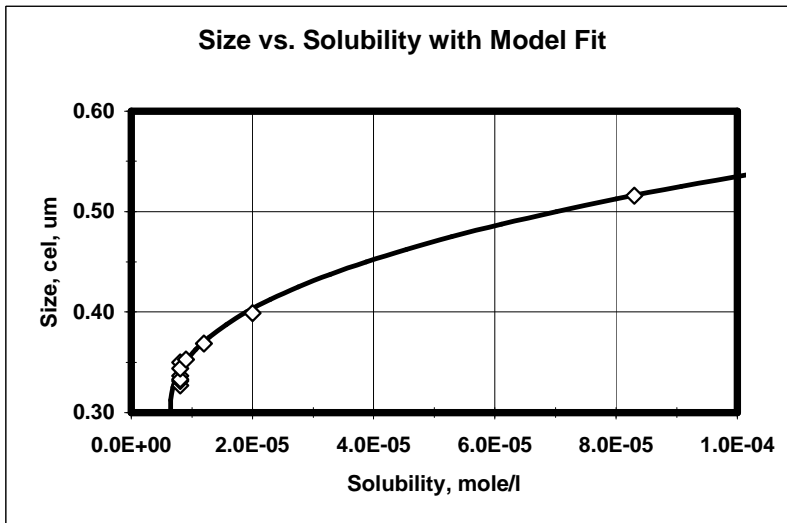


Figure 5 Model: Crystal Size, um, and Model Fit vs. Solubility

The necessary constants to calculate the derive parameters are listed in **Table 8**.

Table 8 Constants for Model Calculations		
Table 5		
Constants for Model Calculations		
Constant	Value	Comment
k_v	1.0	Cubic, volume constant
k_s	6.0	Cubic, surface constant
γ	52.5	erg/cm², ref. 18
D	1.60E-05	cm²/s, ref. 19
V_m	25.9	cm³/mol, AgCl
R_g	8.31E07	erg/deg*mol
	1.987	cal/deg*mol
T	333K/60C	Temperature

The coefficient of L^3 , a_1 , is equal to K , and allows calculating an average value for Ψ of 1.57, (equation (27)). From Ψ , an average of L^*/L to 0.389 was obtained (equation (11)).

Since the average crystal size, L , is available from the experiment, the critical crystal size is calculated for each reaction condition according to equation (35).

	$L^* = 0.389 * L$	(35)
--	-------------------	-------------

From L^* , the critical crystal size, S^* , the supersaturation ratio, was calculated for each reaction condition using equation (15).¹⁷ The coefficients of L^3 , a_1 , and of L^2 , a_2 , were used to calculate the average maximum growth rate G_m to 8.52A/s (equation (28)).

The results of the model calculation, G_m , the average maximum growth rate, Ψ , average stability constant, the S^* -factor, and the R_n/R_i Reactant Split factor are collected in **Table 9**. The S^* - and R_n/R_i factors were used to calculate S^* and R_n/R_i for each experiment.

Table 9	Model Results: G_m , Ψ , L/L^* , S^* -factor, R_n/R_i Reactant Split factor
----------------	--

Table 6		
Calculated Model Parameters		
Parameter	Value	Comment
G_m	8.52 (A/s)	Maximum Growth Rate
Ψ	1.57	
L^*/L	0.389	Critical / Average Size
R_n/R_i -Factor	$8.34E-6*(C_s/L^2)$	Ratio of Nucleation to Growth
S^* - Factor	$1.0+9.83E-08/L^*$	Supersaturation Ratio

The experimental and the modeling results are compiled in **Table 10** for all experiments. This includes the calculated results as a function of solubility of critical, L^* , and nascent, crystal size L_n ; the supersaturation Ratio, S^* ; and the reactant split ratios, R_n/R_i , R_n/R_0 , and R_i/R_0 .

Table 10	AgCl Solubility: Critical, L^*, and Nascent, L_n, Crystal Size; Supersaturation Ratio, S^*; and Reactant Split, R_n / R_i, R_n/R_0, and R_i/R_0
-----------------	--

Table 7								
Derived Parameters: Critical, L^* and Nascent, L_n Crystal Size; Supersaturation Ratio, S^*; and Reactant Split Ratios, R_n/R_i, R_n/R_0, R_i/R_0								
pAg	Solubility	Size (cel)	L^*	L_n	S^*	R_n/R_i	R_n/R_0	R_i/R_0
	mole/l	μm	μm	μm				
7.8	8.30E-05	0.516	0.201	0.305	1.0049	0.260	0.207	0.793
7.1	2.00E-05	0.399	0.155	0.182	1.0063	0.105	0.095	0.905
6.4	8.10E-06	0.337	0.131	0.129	1.0075	0.060	0.056	0.944
6.4	8.10E-06	0.327	0.127	0.128	1.0077	0.063	0.059	0.941
6.4	8.10E-06	0.350	0.136	0.131	1.0072	0.055	0.052	0.948
6.4	8.10E-06	0.331	0.129	0.128	1.0076	0.062	0.058	0.942
6.4	8.10E-06	0.333	0.130	0.128	1.0076	0.061	0.057	0.943
6.4	8.10E-06	0.344	0.134	0.130	1.0073	0.057	0.054	0.946
5.9	9.00E-06	0.353	0.137	0.136	1.0072	0.060	0.057	0.943
5.4	1.20E-05	0.369	0.143	0.151	1.0069	0.074	0.069	0.931
pAg 6.4	Average	0.337	0.131	0.129	1.0075	0.060	0.056	0.944
	Std. Dev.	0.009	0.003	0.001	0.0002	0.003	0.003	0.003

Experimental, critical, and nascent crystal sizes, L , L^* , and L_n

The experimental, critical, and nascent crystal sizes, L , L^* , and L_n , are plotted vs. solubility in Figure 6. All crystal size types increase with increasing solubility. The critical and nascent crystal sizes are significantly smaller than the average crystal size. At the lowest solubility, L^* and L_n are virtually equal. Above the minimum solubility, the nascent crystal size, L_n , is larger

than the critical crystal size, L^* , and their separation increases with solubility. The critical crystal size, L^* , has equal probability to grow or dissolve under the reaction conditions. Thus the nascent crystal size, L_n , has a higher than equal probability to grow. The modeling results are thus in agreement with the expectations.

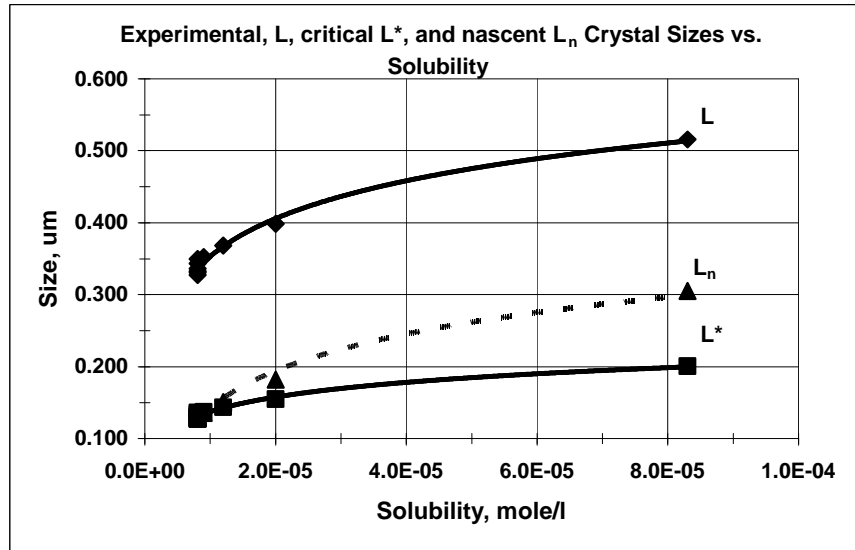


Figure 6	Sizes of experimental, L, critical, L^* , and nascent, L_n Crystal Size vs. Solubility
----------	--

Supersaturation Ratio, S^*

The supersaturation ratio, S^* , is plotted vs. solubility in Figure 7. The value of S^* decreases with increasing solubility.

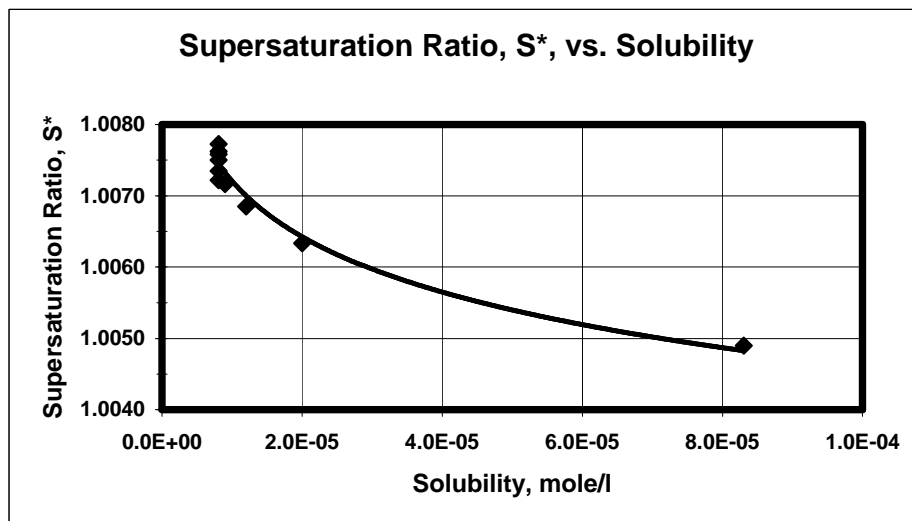


Figure 7	Supersaturation Ratio, S^* , vs. Solubility
----------	---

The supersaturation ratio for the experiments spans a range of 1.0049 to 1.0077. Lower supersaturation ratios were associated with higher solubility. The range indicates that the supersaturation is 0.49 to 0.77 percent higher than the saturation solubility.

Reactant Split Ratios, R_n/R_i , R_n/R_0 , and R_i/R_0

The reactant split ratios, R_n/R_i , R_n/R_0 , and R_i/R_0 are shown as a function of solubility in Figure 8, and in Table 10. The plot shows that the reactant split increases with increasing solubility. This indicates that at higher solubility more reactant goes into nucleation and less into crystal growth. This may be related to the observation that the nascent crystal size, L_n , increases with solubility, and thus more of the incoming reactant stream is needed for nucleation (Figure 8).

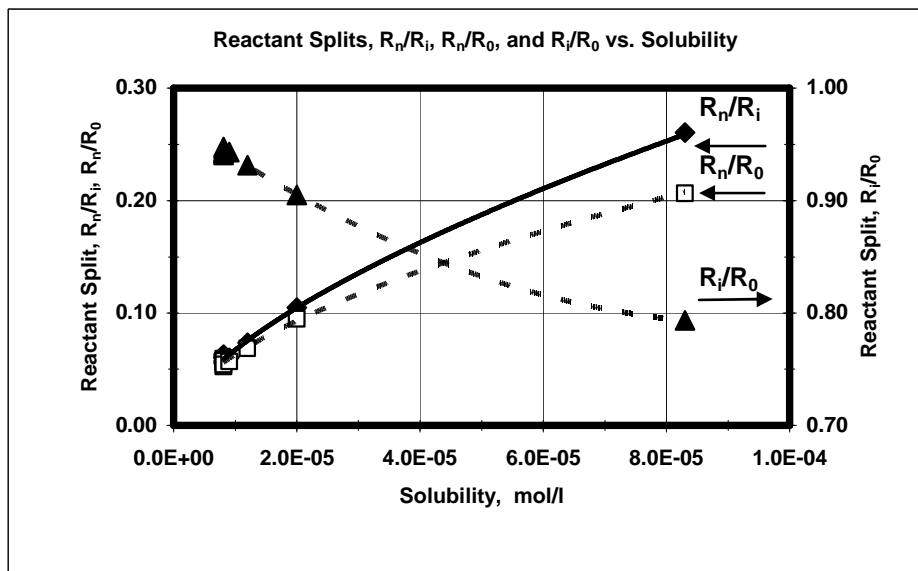


Figure 8	Reactant Split Ratios, R_n/R_i , R_n/R_0 , and R_i/R_0 vs. Solubility
----------	---

VI. Conclusions

The extension of the BNG model to the CSTR crystallizer resulted in an equation that relates crystal size and reaction conditions and is free of arbitrary parameters. In the present study, the correlation between crystal size and solubility was explored for the continuous precipitation of silver chloride. The values of two parameters, which are initially not known, Ψ , a factor related to the supersaturation ratio, and, G_m , the maximum growth rate, are obtained from the combination of model and experiments. The value of Ψ allows calculating the supersaturation during steady state, and thus has a defined physical meaning. Individual values of G_m and Ψ for

each solubility condition may be obtained by selectively designing solubility conditions. In the context of the present experiments, such data were not available, and average values of Ψ and G_m were obtained.

For the silver chloride system, the average maximum growth rate, G_m , was determined to 8.52 $\mu\text{m/s}$. The average of the parameter Ψ was determined to 1.57. It is directly related to the ratio of critical to average crystal size, L^*/L (equation (11)), from which the critical crystal size L^* was obtained (range 0.137 – 0.201 μm). The critical crystal size, L^* , is related to the supersaturation at steady state which was calculated to vary between 1.0049 and 1.0075. L^* increases with solubility.

The model allows calculating the size of the nascent crystals, L_n , which are the initial stable crystals during the nucleation process. The size of L_n was determined to increase with solubility from 0.129 to 0.305 μm , and is larger than L^* .

The reactant split ratio of incoming reactant used for nucleation and growth could be determined using the present model. The ratio of R_n/R_i increased from 0.060 to 0.260 with increasing solubility. From this ratio the fraction of R_n and R_i vs. R_0 , the incoming reaction stream, could be calculated and are reported (R_n/R_0 and R_i/R_0).

The model predicts that the average crystal size is independent of reactant addition rate, suspension density, and reaction volume. This prediction was confirmed for precipitations where the reaction addition rate was varied from 0.005 to 0.04 mol/min, resulting in a variation of suspension density from 0.05 to 0.4 mole/l. These experiments gave an invariant average crystal size of 0.337 (+/- 0009) μm . A doubling of the reaction volume from 300 to 600 mL for constant suspension density of 0.1mole/L gave the same crystal size and crystal number within the limits of error. This confirms the independence of crystal size from reaction volume.

The predicted third order correlation between solubility and crystal size was confirmed (correlation coefficient $R=0.9996$). Since the AgCl solubility goes through a minimum and does not include zero solubility, an intercept was included, which represents the solubility where the crystal size is extrapolated to zero ($L=0$). The zero-size condition cannot be obtained for the precipitation of AgCl.

The present experiments confirm the predictions of the BNG based model for continuous crystallization for the correlation between crystal size and crystal solubility. These results add to the previous confirmation of the predictions for the size dependence on residence time, τ . Together, these confirmations of the BNG based continuous crystallization model make it a useful model to correlate crystal size to variations of precipitation conditions.

The BNG based continuous crystallization model correctly predicts and quantitatively correlates the crystal size-dependence on solubility and suspension density in the CSTR crystallizer without the need for arbitrary adjustable parameters. It also allowed determining important reaction parameters that were previously not accessible.

Table 1		
Constants for AgCl Solubility Calculation		
Component	$K_{m,n}$	ΔH
	(25C)	(kcal/mole)
$[Ag^+]$	10^{-pAg}	
$[AgCl]$	$10^{-3.3}$	-2.7
$[AgCl_2^-]$	$10^{-5.25}$	-3.9
$[AgCl_3^{2-}]$	$10^{-5.7}$	-5.8
$[AgCl_4^{3-}]$	$10^{-5.4}$	-13.9
$K_{sp} = [Ag^+][Cl^-]$	$K_{m,n} = \frac{[Ag^+]^m [Cl^-]^n}{[Ag_m Cl_n]^{m-n}} ; n=1$	
$\log K_{sp} = -(3206 \pm 42) / T + (1.17 \pm 0.14)$		
$T(K) = 273.15 + degC$		

Table 2	
Reference CSTR Precipitation Procedure for AgCl	
300 ml Reaction Volume (CSTR Crystallizer)	
2.4% Gelatin in distilled Water	
60 degree C	
EMF = 170mV, silver vs. silver/silver chloride (4.0N KCl) reference electrode*	
3.0 min Residence time	
10 ml/min Reactant Flow Rate (AgNO₃, NaCl)	
1.0 Mole/L Reactant Concentration	
80 ml/min Gelatin Flow Rate	
0.10 Mole/L AgCl Suspension Density	
Samples were collected after 12 residence times	
Crystal Size Analysis by Joyce-Loebl Disc Centrifuge	
The solubility was adjusted with sodium chloride to aim pAg	
* pAg = $\frac{(599 - mV) - (T - 25) * 0.129}{(273 + T) * 0.198}$	T= degC, mV= EMF

Table 3						
Experimental Results: Crystal Size and Number						
pAg	Reaction Volume mL	Reactant Concentr. Mol/L	Reactant Flow Rate mL/min	Suspension Density M/L	Size cel μm	Crystal Number $Z \cdot E+14$
7.8	300	1.0	10	0.100	0.516	0.19
7.1	300	1.0	10	0.100	0.399	0.41
6.4	300	0.5	10	0.050	0.327	0.37
6.4	600	1.0	20	0.100	0.337	0.68
6.4	300	1.0	10	0.100	0.350	0.60
6.4	300	2.0	10	0.200	0.331	1.42
6.4	300	3.0	10	0.300	0.333	2.10
6.4	300	4.0	10	0.400	0.344	2.55
5.9	300	1.0	10	0.100	0.353	0.59
5.4	300	1.0	10	0.100	0.369	0.52

Table 4				
Suspension Density Variations at pAg6.4 : Crystal Size and Number				
Reactant Concentr.	Reaction Volume	Suspension Density	Crystal Size cel	Crystal Number
Mole/l	ml	Mole/l	µm	Z*E14
0.05	300	0.05	0.327	0.37
0.10	600	0.10	0.337	0.68
0.10	300	0.10	0.350	0.60
0.20	300	0.20	0.331	1.42
0.30	300	0.30	0.333	2.10
0.40	300	0.40	0.344	2.55

Table 8		
Constants for Model Calculations		
Constant	Value	Comment
k_v	1.0	Cubic, volume constant
k_s	6.0	Cubic, surface constant
γ	52.5	erg/cm², ref. 19
D	1.60E-05	cm²/s, ref. 19
V_m	25.9	cm³/mol, AgCl
R_g	8.31E07	erg/deg*mol
	1.987	cal/deg*mol
T	333K/60C	Temperature

Table 9		
Calculated Model Parameters		
Parameter	Value	Comment
G_m	8.52 (A/s)	Maximum Growth Rate
Ψ	1.57	
L^*/L	0.389	Critical / Average Size
R_n/R_i -Factor	$8.34E-6*(C_s /L^2)$	Ratio of Nucleation to Growth
S^* - Factor	$1.0+9.83E-08/L^*$	Supersaturation Ratio

Table 10								
Derived Parameters: Critical, L^* and Nascent, L_n Crystal Size; Supersaturation Ratio, S^*; and Reactant Split Ratios, R_n/R_i, R_n/R_0, R_i/R_0								
pAg	Solubility	Size (cel)	L^*	L_n	S^*	R_n/R_i	R_n/R_0	R_i/R_0
	mole/l	μm	μm	μm				
7.8	8.30E-05	0.516	0.201	0.305	1.0049	0.260	0.207	0.793
7.1	2.00E-05	0.399	0.155	0.182	1.0063	0.105	0.095	0.905
6.4	8.10E-06	0.337	0.131	0.129	1.0075	0.060	0.056	0.944
6.4	8.10E-06	0.327	0.127	0.128	1.0077	0.063	0.059	0.941
6.4	8.10E-06	0.350	0.136	0.131	1.0072	0.055	0.052	0.948
6.4	8.10E-06	0.331	0.129	0.128	1.0076	0.062	0.058	0.942
6.4	8.10E-06	0.333	0.130	0.128	1.0076	0.061	0.057	0.943
6.4	8.10E-06	0.344	0.134	0.130	1.0073	0.057	0.054	0.946
5.9	9.00E-06	0.353	0.137	0.136	1.0072	0.060	0.057	0.943
5.4	1.20E-05	0.369	0.143	0.151	1.0069	0.074	0.069	0.931
pAg 6.4	Average	0.337	0.131	0.129	1.0075	0.060	0.056	0.944
	Std. Dev.	0.009	0.003	0.001	0.0002	0.003	0.003	0.003

Table 11		
Glossary of Terms		
Variable	Definition	Comment
Ψ	$L/L^* - 1.0$	
τ	Residence time	Min, sec
C_0	Solubility for $L=0$ (extrapolated)	Mol/L
C_m	Minimum Solubility	
C_s	Solubility	mol/ cm³
D	Diffusion constant	cm²/s
γ	Surface energy	erg/ cm²
G	Crystal growth rate	dL/dt
G_m	Maximum crystal growth rate	cm/s, nm/s
k_s	Crystal surface constant	Cubic: 6.0
k_v	Crystal volume constant	Cubic: 1.0

L	Crystal size	cm, μm
L*	Critical crystal size	cm, μm
L_n	Nascent crystal size	cm, μm
pAg	$-\log [\text{Ag}^+]$	
R_g	General gas constant	erg/deg*mol
S	Supersaturation	Mol/L
S*	Supersaturation ratio	
T	Temperature	K
V	Reaction volume	mL
V_m	Molar volume	cm³ /mol AgCl
Z	Crystal Number	

Figure Captions	
Figure 1	CSTR Crystallization of AgBr: Size Distribution and Randolph – Larson plot
Figure 2:	BNG-Model for Continuous Crystallization
Figure 4	AgCl Solubility and Crystal Size vs. pAg ($-\log[\text{Ag}^+]$)
Figure 5	Model: Crystal Size and Model Fit vs. Solubility
Figure 6	Size, L, critical size, L^* , and nascent size, L_n vs. Solubility
Figure 7	Supersaturation Ratio, S^* , vs. Solubility
Figure 8	Reactant Split Ratios, R_n/R_i , R_n/R_0 , and R_i/R_0 vs. Solubility

Table Captions	
Table 1	Constants for AgCl Solubility Calculations
Table 2	Reference CSTR Precipitation Procedure for AgCl
Table 3	Experimental Results: Crystal Size and Number
Table 4	Suspension Density Variations at pAg6.4: Crystal Size and Number
Table 8	Constants for Model Calculations
Table 9	Calculated Model Results
Table 10	Derived Parameters: Critical, L^* and nascent, L_n crystal size; Supersaturation ratio, S^* ; Reactant Split Ratios R_n/R_i , R_n/R_0 , and R_i/R_0
Table 11	Glossary of Terms

Table of Contents

T a b l e o f C o n t e n t s	
	The Randolph-Larson Model
II.	The BNG Model for the CSTR System
	The BNG Model
	Crystal Growth
	Crystal Nucleation
	The Model
	Supersaturation Ratio
	Reactant Split, R_n and R_i
	Nascent Nucleus Size
	Summary of Model
III.	Size Control by Crystal Solubility
	The Solubility Model
	Solubility
IV.	Experimental
V.	Results
	Suspension Density
	Size-Solubility Correlation
	Experimental, critical, and nascent crystal sizes, L ,
	Supersaturation Ratio, S^*
	Reactant Split Ratios, R_n/R_i , R_n/R_0 , and R_i/R_0
VI.	Conclusions
	Table Captions
	Table 1

Constants for AgCl Solubility Calculations
Table 2
Reference CSTR Precipitation Procedure for AgCl...
Table 3
Experimental Results: Crystal Size and Number
Table 4
Table 8
Constants for Model Calculations
Table 9
Calculated Model Results
Table 10
Derived Parameters: Critical, L^* and nascent, L_n crys
Table 11
Glossary of Terms
Table of Contents
Synopsis:.....

Synopsis:

Crystallization in the continuous stirred tank reactor (CSTR, MSMPR) crystallizer was modeled using the balanced nucleation and growth (BNG) theory. This model was previously supported for predictions related to residence time of AgCl precipitations. The model predictions were now experimentally evaluated for the dependence of size on solubility in the AgCl system. Values of average maximum growth rate, ratio of critical to stable crystal size, critical crystal size, nascent crystal size, supersaturation ratio, and reactant-split ratios into nucleation and growth were obtained from the combination of the model with experimental results. The model correctly predicted the independence of crystal size from suspension density, reaction volume, and reaction addition rate. The BNG based continuous crystallization model thus correctly predicted and quantitatively correlated the crystal size-dependence on solubility in the CSTR crystallizer without the need for arbitrary adjustable parameters. It allowed determining important reaction parameters that were previously not accessible.

References

- (1) Leubner I. H., Crystal Formation (Nucleation) under Kinetically and Diffusion Controlled Growth Conditions, *J. Phys. Chem.* 1987, 91, 6069
- (2) Leubner, I. H., Crystal Formation (Nucleation) in the Presence of Ostwald Ripening Agents, *J. Imaging Science* **1987**, 29, 31
- (3) Leubner, I. H., Crystal Formation (Nucleation) in the Presence of Growth Restrainers, *J. Crystal Growth* **1987**, 84, 496
- (4) Bransom H.S.; Dunning W. J.; Millard B., *Disc. Faraday Soc.* **1949**, 5, 83
- (5) Randolph A.D.; Larson M.A., *AICHE J.* **1962**, 8, 639
- (6) Randolph A.D.; Larson M.A., *Theory of Particulate Processes*, 2nd edition, Academic Press, San Diego, CA, **1991**
- (7) Leubner I.H., A New Crystal Nucleation Theory for Continuous Precipitation of Silver Halides, *J. Imaging Science and Technology*, **1998**, 42, 355
- (8) Leubner I.H., Seeded Precipitations in the Continuous Stirred Tank Reactor Crystallizer, *J. Dispersion Science and Technology* **2001**, 22, 373
- (9) Leubner, I. H. Crystal Growth and Renucleation, Theory and Experiments, *J. Imaging Sci. Technol.* **1993**, 37, 510
- (10) Leubner I. H., Balanced Nucleation and Growth Model for Controlled Crystal Size Distribution, *J. Dispersion Science and Technology* **2002**, 22, 577

-
- (11) Leubner I. H., Particle Nucleation and Growth Models, Current Opinions I Colloid and Interface Science **2000**, 5, 151
- (12) Leubner I. H., Crystal Formation (Nucleation) under Kinetically and Diffusion Controlled Growth Conditions, J. Phys. Chem. **1987**, 91, 6069
- (13) Chateau H.; Pouradier J.; Berry C. R., in The Theory of the Photographic Process, 3rd Edition, T. H. James, Ed., Macmillan, New York, **1971**, p. 6; Pouradier J. et al., J. Chim. Phys., 1954, 51, 375; Towns, M.B. et al., J. Phys. Chem. 1960, 64, 1861; Greeley W. et al., ibid. 1960, 64, 652
- (14) Pouradier J.; Pailliotet A., and Berry C. R., in The Theory of the Photographic Process, 4th Edition, T. H. James, Ed., Macmillan, New York, **1977**
- (15) Wey J. S.; Leubner I. H.; Terwilliger J. P., Transient Behavior of Silver Bromide Precipitation in a Continuous Suspension Crystallizer, Photogr. Sci. Eng. **1983**, 27, 35
- (16) King T.W., Shor S.M., and Pitt D.A., Photogr. Sci. Eng. (1981), 25, 70
- (17) Leubner I. H., Formation of Silver Halide Crystals in Double-Jet Precipitations: AgCl, J. Imaging Science **1985**, 29, 219
- (18) Strong R. W.; Wey J. S., Photogr. Sci. Eng. **1979**, 23, 344
- (19) Strong R. W.; Wey J. S., Photogr. Sci. Eng. **1979**, 23, 344